Finite Element Elasto-Plastic Analysis of Thin Walled Structures of Reinforced Concrete as Applied to Reactor Facilities

F. Fujita*, O. Isobata**
Shimizu Construction Co., Ltd., 4-17 Etchujima-3, Koto-ku, Tokyo 135, Japan
** Nuclear Power Dept.*
*** Research Laboratory*

S. Kawamata
Tohoku Institute of Technology, Sendai-shi 982, Japan

Y. Tsuboi
University of Tokyo, 22-1, Roppongi 7-chome, Minato-ku, Tokyo 106, Japan

SUMMARY

As the reactor facilities become greater in scale and severer in loading conditions, static analysis of structures beyond the elastic limit seems to have rolls of growing importance. As for reinforced concrete structures, the method of elasto-plastic analysis allowing for cracking in concrete has been successfully developed for various types of structures. Nowadays the elasto-plastic finite element analysis of R/C structures provides us with an indispensable tool to assess the ultimate capacity of structures in reactor facilities.

The purpose of this paper is to present a new model of finite element developed for elasto-plastic analysis of R/C shells and to show examples of its application to concrete containments and box-wall structures in a reactor building. The results of the analysis are compared to those from model tests.

As the finite element for thin shells, which seems to be the simplest one within an acceptable accuracy, a quadrilateral element composed of four triangular flat elements is adopted. For each component triangle, the ordinary plane stress formulation in the constant strain field and the one similar to the Morley model in plate bending in the deflection field of constant curvature are also adopted. After the elimination of the freedom of central part, the element has 16 degrees of freedom in the total.

Another characteristic of this elasto-plastic model is incorporation of orthotropic constitutive relation for concrete, which was proposed by one of the authors and successfully applied to analyses of RC wall and PCRVs. To evaluate both the in-plane and bending stiffness of the elements beyond the elastic limit or after cracking of concrete, so-called "layered approach" was applied. Major assumptions in the analysis are as follows: a) Kirchhoff-Love's hypotheses are valid at any step. b) Concrete section is divided into some imaginary layers, and each layer is in the state of plane stress. c) Concrete under a biaxial stress state is idealized as an orthotropic material in which elastic moudli are variable. d) Crack is governed by the uniaxial tensile strength and compressive failure follows octahedral shear failure criterion. e) Steel is treated by a bilinear model.

An iteration procedure using a tangent stiffness is applied for each incremental loading step. Residual forces caused by cracking and material nonlinearity are released in each loading step. This method is applied to the test models of cylindrical containments and box-wall structures of reinforced concrete. In comparison between the calculation and the measurements, the applicability and the validity of the proposed method are investigated.

1. Introduction

In the design of reactor facilities, elasto-plastic analysis of reinforced concrete structures is an indispensable tool to investigate their behavior beyond the elastic limit and ultimate bearing capacity. Development of finite element analysis of reinforced concrete with material nonlinearity was traced in a survey paper by Bergan and Holand[1].

In the effort of research and development of concrete containment vessels, the authors developed a new program of elasto-plastic analysis of reinforced concrete shells, in which the simplest model of shell element and an orthotropic constitutive relation are adopted, and verified its validity with reference to the results of model experiments of containers and box-wall structures with various loading conditions.

The basic element for the elasto-plastic analysis is a flat triangular shell element of assumed displacement type. It is formed by the combination of a constant strain in-plane element and a constant curvature plate bending element, the latter containing normal slopes of edges as nodal parameters. The actual analysis utilizes a quadrilateral element of 16 degrees of freedom formed by combination of four triangular basic elements, with the interior degrees of freedom eliminated.

For the two-dimensional stress-strain relationship of concrete, an orthotropic nonlinear formula proposed by one of the authors[2] was adopted. For concrete, the octahedral shear failure and tension cut-off criteria were also imposed. The Kirchhoff-Love's assumptions were assumed to be valid for the whole range of the analysis and the layered approach of elasto-plastic stiffness evaluation.

In this paper, derivation of the shell element is outlined with examination of its accuracy in elastic range and the assumption of elasto-plastic material property and the procedure of nonlinear analysis are described.

As examples, the method is applied to the analysis of a cylindrical container and a box-wall structure. Comparison of the computed results with the corresponding experimental data indicates the applicability of the proposed method.

2. Shell Element and Its Accuracy in Elastic Range

As a basic unit, we take a flat triangular shell element. Because of flatness, in-plane stiffness and bending stiffness can be separately formulated and straight combined. For the former, we adopt the well-known constant strain plane stress element having six corner node degrees of freedom. For the latter, we introduce the simplest plate bending model of assumed displacement type, i.e. a triangular element whose nodal parameters are corner node deflection, w_i (i=1,2,3), and rotation of normal slope at the middle points of three edges, $\left.\frac{\partial w}{\partial n}\right|_j$ (j=4,5,6). Referring to Fig. 1, let the nodal parameter be defined by

$$\{f_b\} = (f_{z1}\ f_{z2}\ f_{z3}\ \vdots\ M_{n4}\ M_{n5}\ M_{n6})^T, \tag{1.a}$$

$$\{d_b\} = (w_1\ \ w_2\ \ w_3\ \vdots\ w,_{n4}\ w,_{n5}\ w,_{n6})^T \tag{1.b}$$

We assume the following shape function of w in terms of area coordinate:

$$w = \alpha_1\zeta_1+\alpha_2\zeta_2+\alpha_3\zeta_3+\alpha_4\zeta_1\zeta_2+\alpha_5\zeta_2\zeta_3+\alpha_6\zeta_3\zeta_1 \tag{2}$$

The vector of curvature

$$\{\bar{\kappa}\} = (\kappa_x\ \kappa_y\ \kappa_{xy})^T = (-\frac{\partial^2 w}{\partial x^2}\ -\frac{\partial^2 w}{\partial y^2}\ -2\frac{\partial^2 w}{\partial x \partial y})^T \tag{3}$$

is first related to the parameter $\{\alpha\}$ in the forms of derivatives of w with respect to ζ_i (i=1,2), which are then transformed to x-y coordinate system,

i.e. $$\{\bar{\kappa}\} = [B^\alpha]\{\alpha\} \tag{4}$$

where $$\{\alpha\} = (\alpha_1\ \alpha_2\ \alpha_3\ \alpha_4\ \alpha_5\ \alpha_6)^T \ , \tag{5}$$

$$[B^\alpha] = \frac{1}{4A^2}\left[\begin{array}{ccc|ccc} 0 & 0 & 0 & -2y_{31}y_{23} & 2(y_{31}^2+y_{31}y_{23}) & 2(y_{23}^2+y_{31}y_{23}) \\ 0 & 0 & 0 & -2x_{13}x_{32} & 2(x_{13}^2+x_{13}x_{32}) & 2(x_{32}^2+x_{13}x_{32}) \\ 0 & 0 & 0 & \begin{array}{l}-2(x_{13}x_{23} \\ \quad +x_{32}y_{31})\end{array} & \begin{array}{l}4x_{13}y_{31} \\ +2(x_{13}y_{23}+x_{32}y_{31})\end{array} & \begin{array}{l}4x_{32}y_{23} \\ +2(x_{13}y_{23}+x_{32}y_{31})\end{array} \end{array}\right] \tag{6.a}$$

$$x_{ij}=x_i-x_j,\ y_{ij}=y_i-y_j\ , \quad A:\text{area of the element} \tag{6.b}$$

The rotation of normal slope is given by

$$\left.\frac{\partial w}{\partial n}\right|_i = \left[\frac{\partial w}{\partial x}\frac{\partial x}{\partial n}+\frac{\partial w}{\partial y}\frac{\partial y}{\partial n}\right]_i = \cos\theta_i\left.\frac{\partial w}{\partial x}\right|_i+\sin\theta_i\left.\frac{\partial w}{\partial y}\right|_i \ , \quad i=4,5,6 \tag{7}$$

and is written in terms of $\frac{\partial w}{\partial \zeta_i}$ (i=1,2) by the coordinate transformation. Substituting the area coordinate of each node into Eqs. (2) and (7), we can represent the nodal parameters in terms of $\{\alpha\}$, i.e.

$$\{d_b\} = [C]\{\alpha\} = \begin{bmatrix} I & 0 \\ C_{21} & C_{22} \end{bmatrix}\{\alpha\} \tag{8}$$

where I : unit matrix ,

$$C_{21} = \frac{1}{2A}\begin{bmatrix} c_4y_{23}+s_4x_{32} & c_4y_{31}+s_4x_{13} & c_4y_{12}+s_4x_{21} \\ c_5y_{23}+s_5x_{32} & c_5y_{31}+s_5x_{13} & c_5y_{12}+s_5x_{21} \\ c_6y_{23}+s_6x_{32} & c_6y_{31}+s_6x_{13} & c_6y_{12}+s_6x_{21} \end{bmatrix} , \tag{9.a}$$

$$C_{22} = \frac{1}{4A}\begin{bmatrix} c_4y_{23}+s_4x_{32} & c_4y_{32}+s_4x_{23} & c_4y_{23}+s_4x_{32} \\ c_5y_{31}+s_5x_{13} & c_5y_{31}+s_5x_{13} & c_5y_{31}+s_5x_{13} \\ c_6y_{21}+s_6x_{12} & c_6y_{12}+s_6x_{21} & c_6y_{12}+s_6x_{21} \end{bmatrix} , \tag{9.b}$$

$$c_i=\cos\theta_i,\ s_i=\sin\theta_i,\ i=4,5,6 \tag{9.c}$$

By a well-known procedure, the bending part of element stiffness matrix is formulated as

$$[K] = A[C^{-1}]^T[B^\alpha]^T[D][B^\alpha][C^{-1}] \tag{10}$$

where [D] is a matrix of moment-curvature relation of plate.

The plate bending element we derived seemed to be similar to the one developed by L.S.D. Morley[3] and, by test computation of square plates, we found that the both yielded the same results. At the same time, we thought that this simple element was not satisfactory in accuracy. Therefore, we formed a quadrilateral shell element as an assembly of four basic units, where the freedom of five interior nodes was eliminated (Fig. 2). To see the performance of the new element, an elastic cylindrical shell loaded vertically was analyzed (Fig. 3). The results of the test analysis show that the quadri-

lateral shell element of 16 degrees of freedom works well with accuracy sufficient to the purpose (Figs. 4 and 5). The accuracy of the present element seems to be comparable to Herrmann's shell element in mixed formulation [4]. It has also advantage of facilitating the assessment of tangent stiffness because it is based on the assumption of constant strain field.

3. Elasto-plastic Model

3.1 Stress-Strain Relation of Concrete in Plane Stress

Many constitutive models of concrete have been proposed, because the concrete behavior under multi-axial stresses is not so clear as the one of uniaxial stresses. The orthotropic assumption mentioned below provides the freedom that the constitutive equation can be written by more parameters than those in the isotropic body, and it may also represent the behavior after cracking by a single equation.

The authors adopt an orthotropic model where both moduli of elasticity and Poisson's ratios are variable [2]. Let us take principal stress axes as orthotropic axes, and introduce parameters η_i (i=1,2) with respect to two Young's moduli E_i :

$$E_i = \eta_i \cdot E_0 \tag{11}$$

where E_0 is the initial tangent modulus of elasticity.

Then we take parameters ξ_{ij} (i,j=1,2,i≠j) of Poisson's ratios ν_{ij} in the form

$$(\nu_{ij} \cdot \nu_{ji})^{1/2} = \xi_{ij} = \xi_{ji} \tag{12}$$

Therefore, substituting Eqs. (11) and (12) into the stress-strain relationship of the orthotropic medium, the incremental stress-strain matrix is derived as follows:

$$\{\Delta\sigma_c\} = [D_c]\{\Delta\varepsilon\} \tag{13}$$

where

$$[D_c] = \frac{E_0}{1-\xi_{12}^2} \begin{bmatrix} \eta_1 & \xi_{12}\eta_1^{1/2}\eta_2^{1/2} & 0 \\ \xi_{12}\eta_1^{1/2}\eta_2^{1/2} & \eta_2 & 0 \\ 0 & 0 & \frac{(1-\xi_{12}^2)}{E_0} G_{12} \end{bmatrix}, \tag{14.a}$$

$$\{\Delta\sigma_c\} = (\Delta\sigma_1\ \Delta\sigma_2\ \Delta\sigma_{12})^T , \tag{14.b}$$

$$\{\Delta\varepsilon\} = (\Delta\varepsilon_1\ \Delta\varepsilon_2\ \Delta\varepsilon_{12})^T \tag{14.c}$$

Now we approximate the uniaxial stress-strain relationship in the form of

$$\sigma_i = F(\varepsilon_i) = C_1 E_0 \varepsilon_i / \{|(\varepsilon_i/\varepsilon_c)^3| + C_2|(\varepsilon_i/\varepsilon_c)| + C_1\} \tag{15}$$

where C_1 and C_2 are experimental constants, ε_c being the strain corresponding to the uniaxial compressive strength σ_c (Fig. 6)

By the definition of Eq. (13), η_i is given as

$$\eta_i = dF(\varepsilon_i)/E_0 d\varepsilon_i \tag{16}$$

We assume that ξ_{12}, the parameter of Poisson's ratio, depends on the principal strains and can be represented by the form of

$$\xi_{12} = \xi(\varepsilon_1, \varepsilon_2) = \{1-(1-2\nu_0)k(\varepsilon_1, \varepsilon_2)\}/2 \tag{17}$$

where

$$k(\varepsilon_1, \varepsilon_2) = \eta_1^{1/2}\eta_2^{1/2}/\{1+d_1\varepsilon_1\varepsilon_2/\varepsilon_c^2 + d_2(\varepsilon_1\varepsilon_2+|\varepsilon_1\varepsilon_2|)/\varepsilon_c^2\} , \tag{18}$$

d_1 and d_2 being experimental constants which conform with the uniaxial and biaxial compressive failure tests, ν_0 the initial value of ξ_{12}.
Shear modulus of elasticity G_{12} in non-crack state is assumed by

$$G_{12} = \eta_1^{1/2}\eta_2^{1/2}E_0/2(1+\xi_{12}) \tag{19.a}$$

For cracked state, we take G_{12}

$$G_{12} = \alpha G_0 \ , \quad 0 < \alpha < 1 \tag{19.b}$$

where α is the empirical constant, and G_0 the initial value of G_{12}.

3.2 Fracture condition

Both cracking and compressive failure are taken into consideration as fractures under biaxial stresses. We assume that the crack occurrs perpendicularly to the principal tensile stress when the latter exceeds the uniaxial tensile strength σ_t. The compressive failure is assumed to follow the octahedral shear failure criterion:

$$\tau_{oct} \geq n\sigma_{oct} + c \tag{20}$$

where τ_{oct} means the octahedral shear stress and σ_{oct} the octahedral normal stress. In the above criterion, the experimental constants n and c are determined by

$$n = -\sqrt{2}(a-1)/(2a-1) \ , \tag{21.a}$$

$$c = -\sqrt{2}a\sigma_c/3(2a-1) \tag{21.b}$$

where a is a parameter representing the strength under uniform biaxial compression defined by $\sigma_1=\sigma_2=a\sigma_c$.

4. Elasto-Plastic Analysis

In the elasto-plastic analysis, so-called "layered approach"[5] is applied, and the following assumptions are adopted.

1) Kirchhoff-Love's hypotheses are valid at any loading step.
2) Concrete section is divided into imaginary layers, and each layer is assumed to be in the state of plane stress.
3) Reinforcement and prestressing steel are idealized by bilinear models (Fig. 6).
4) Reinforcement and prestressing steel are treated as infinitely thin layers having effective stiffness in their direction, and their strains conforming with those of concrete in their position.

The constitutive relation of reinforced concrete section in the x-y coordinate system is derived as follows from the definition of stress resultants and the assumptions in the analysis.

$$\left\{\begin{matrix}\Delta\bar{N}\\ \hline \Delta\bar{M}\end{matrix}\right\} = \left[\begin{matrix}\sum_i[\bar{D}_c]_i\Delta Z_i + \sum_j[\bar{D}_s]_j A_{sj} & \sum_i[\bar{D}_c]_i Z_i\Delta Z_i + \sum_j[\bar{D}_s]_j Z_{sj}A_{sj}\\ \hline \sum_i[\bar{D}_c]_i Z_i\Delta Z_i + \sum_j[\bar{D}_s]_j Z_{sj}A_{sj} & \sum_i[\bar{D}_c]_i Z_i^2\Delta Z_i + \sum_j[\bar{D}_s]_j Z_{sj}^2A_{sj}\end{matrix}\right]\left\{\begin{matrix}\Delta\bar{\varepsilon}_0\\ \hline \Delta\bar{\kappa}\end{matrix}\right\} \tag{22}$$

where

$$\{\Delta\bar{N}\} = (\Delta N_x \ \Delta N_y \ \Delta N_{xy})^T, \quad \{\Delta\bar{M}\} = (\Delta M_x \ \Delta M_y \ \Delta M_{xy})^T \tag{23.a}$$

$$\{\Delta\bar{\varepsilon}_0\} = (\Delta\varepsilon_{x0} \ \Delta\varepsilon_{y0} \ \Delta\varepsilon_{xy0})^T, \quad \{\Delta\bar{\kappa}\} = (\Delta\kappa_x \ \Delta\kappa_y \ \Delta\kappa_{xy})^T \tag{23.b}$$

top bar means value in the x-y coordinate system, $[\bar{D}c]i$ is the constitutive matrix of ith concrete layer and $[\bar{D}s]j$ the one of jth steel layer. Z_i and Z_{sj} are the distances of the concrete layer and steel layer respectively from the reference surface. ΔZ_i and A_{sj} are thickness of concrete layer and area of steel section a unit length.

In prestressed concrete structures, prestressing members are treated as reinforcements with initial stresses.

An iteration procedure using a tangent stiffness is applied for each incremental loading step. Incremental constitutive coefficients of shell section are evaluated based on Eq. (22) in which those of concrete and steel layers are updated for each loading step. After tangent stiffnesses of four constituent triangular elements are calculated, that of a quadrilateral element is evaluated in the same manner as in the elastic analysis. Residual nodal forces caused by cracking and material nonlinearity are released in each step.

5. Numerical Examples

The first example is a case of axi-symmetric problem. Shell wall ends of reinforced concrete containment vessel subjected to the internal pressure were tested to clear the resistance mechanism of transverse shear at the wall bottom (Fig. 8). The present method was applied to analyze the nonlinear behavior of these models. Fig. 9 shows that analytical defections simulate bilinear behaviors of the test models. Fig. 10 shows transverse shear at the wall bottom. Transverse shear in the analysis increases after vertical cracking and is close to constant after yielding of reinforcement at the bottom, while the experimental resuslt increases monotonically. There is a difference which was produced by the non-axisymmetric behaviors of the test models caused by a large deformation with cracking and yielding. Fig. 11 shows analytical bending moment distributions.

As another example, a box-wall structure subjected to lateral loads such as applied to reactor facilities was analyzed (Fig. 12). Analytical results have a good agreement with experimental ones with respect to deflection, strain and cracking pattern.

6. Conclusions

A quadrilateral element composed of four triangular elements in which strains and curvatures are constants is introduced to study the elasto-plastic behaviors of R/C shells. The accuracy of the present element is examined, and it is verified that the element has a good accuracy in practical usage.

In elasto-plastic analysis, "layered approach" is adopted, and concrete constitutive relation of each layer is idealized as the orthotropic medium where modulus of elasticity and Poisson's ratio are parameters.

This method is applied to the test models of thin walled structures such as applied to reactor facilities. Analytical results showed a good agreement with the experiments. Therefore it is confirmed that this method is of practical value in the prediction of elasto-plastic behaviors of thin walled reinforced concrete structures and prestressed concrete structures.

References

[1] P.G. Bergan and I. Holand, "Nonlinear Finite Element Analysis of Concrete Structures", Computer Methods in Applied Mechanics and Engineering, 17/8, 1979

[2] O. Isobata, "An Empirical Study of Nuclear Reactor Vessel", 2nd US-JAPAN Seminar on HTGR Safety Tecnology, Fuji, Japan, Nov. 1978

[3] L.S.D. Morley, "The Constant-Moment Plate-Bending Element", J. of Strain Analysis, Vol. 6, No. 1, 1971

[4] L.R. Herrmann, "A Finite Element Analysis for Thin Shells", AIAA J., Vol. 6, No. 10, 1968

[5] C.S. Lin, "Nonlinear Analysis of Reinforced Concrete Slabs and Shells", Structures and Materials Research, No. UC SESM73-7, Dept. of Civil Engineering, University of California, April 1973

TABLE 1 Data for Analysis of R/C Shell Wall Ends

MODEL	E_o (kg/cm^2)	V_o	σ_c (kg/cm^2)	σ_t (kg/cm^2)	ε_c (%)	REINFORCEMENT RATIO (%)	
						VERTICAL	HOOP
I	186,000	0.17	-240	20.8	-0.24	1.11	0.88
II	210,000	0.16	-277	21.3	-0.24	0.55	0.88
E_s = 2,100,000 kg/cm^2, σ_y = 3,900 kg/cm^2, β = 0.04							
η_c = 0.1, d_1 = 5, d_2 = 2.5, a = 1.1, c = -0.432 σ_c, n = -0.118							

TABLE 2 Data for Analysis of R/C Box-Wall Structure

E_o (kg/cm)	V_o	σ_c (kg/cm^2)	σ_t (kg/cm^2)	ε_c (%)	REINFORCEMENT RATIO (%)	
					VERTICAL	HORIZONTAL
183,000	0.16	-257	23.6	-0.24	1.15	1.15
E_s = 1,910,000 kg/cm^2, ε_y = 3,950 kg/cm^2, β= 0.04						
η_c = 0.1, d_1 = 5, d_2 = 2.5, a = 1.1, c = -0.432 σ_c, n = -0.118						

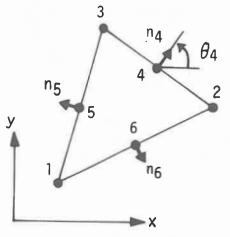

Fig.1 Constant Curvature Plate Bending Element

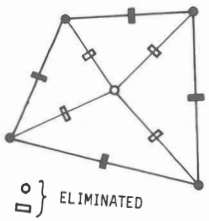

Fig.2 Quadrilateral Shell Element

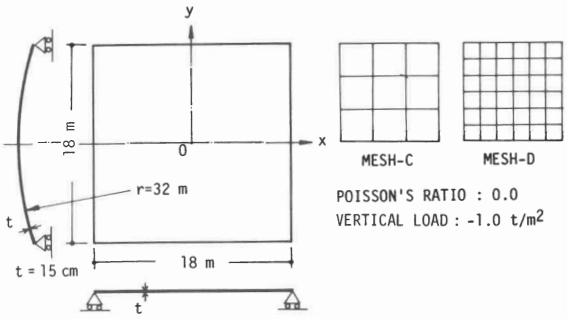

Fig.3 Cylindrical Shell Model

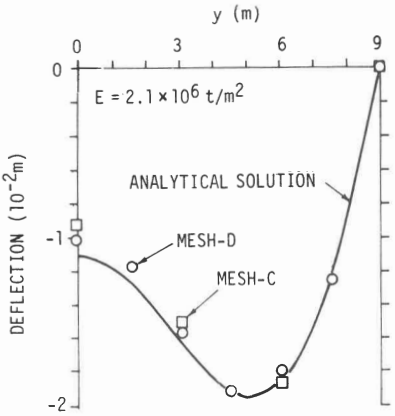

Fig.4 Vertical Deflection at x=0

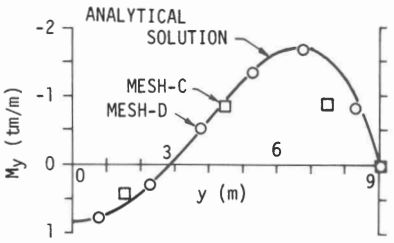

Fig.5 Bending Moment My at x=0

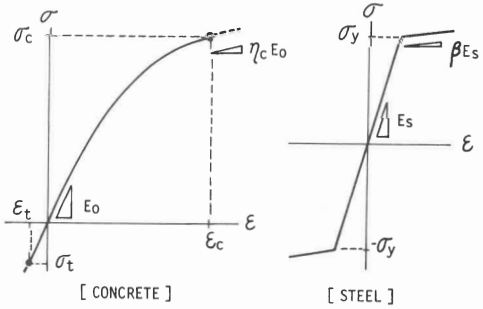

Fig.6 Stress-Strain Relation

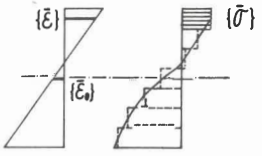

Fig.7 Strain and Stress

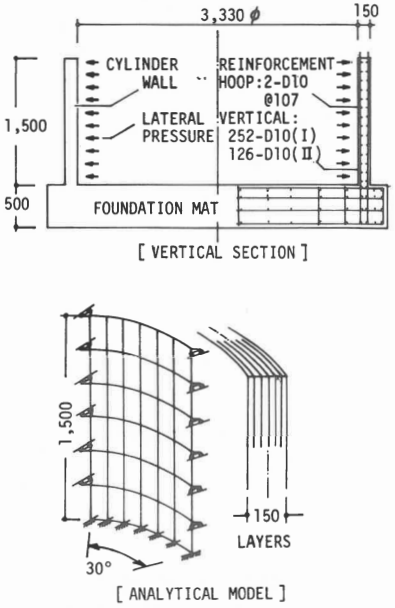

Fig.8 Testing Model of Containment and Analytical Model

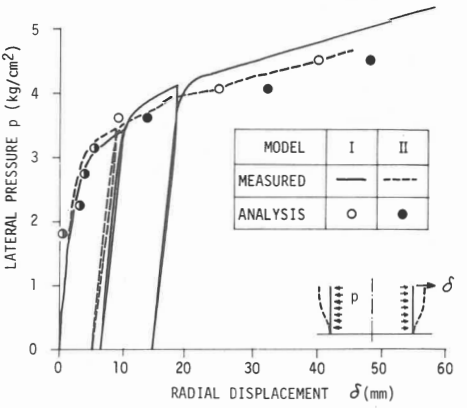

Fig.9 Pressure-Radial Displacement

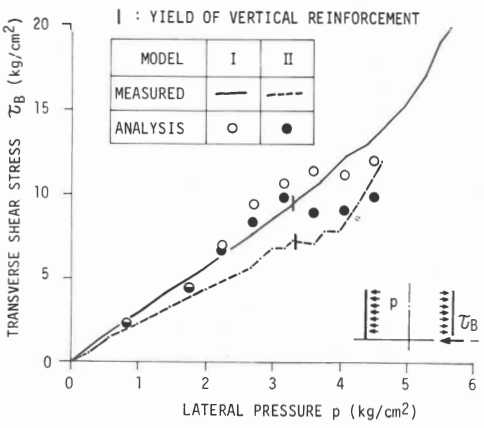

Fig.10 Transverse Shear Stress at The Wall Bottom

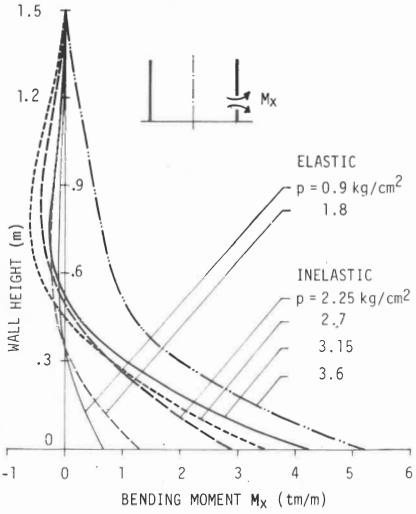

Fig.11 Bending Moment in Vertical Direction(Model I)

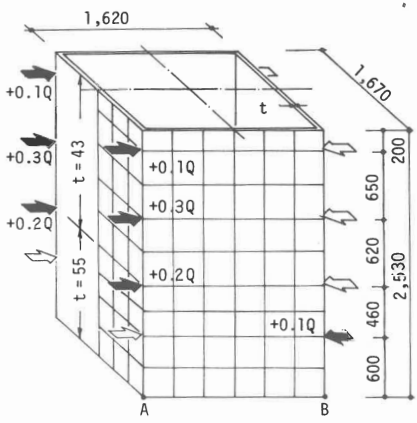

Fig.12 Box-Wall Structure Model

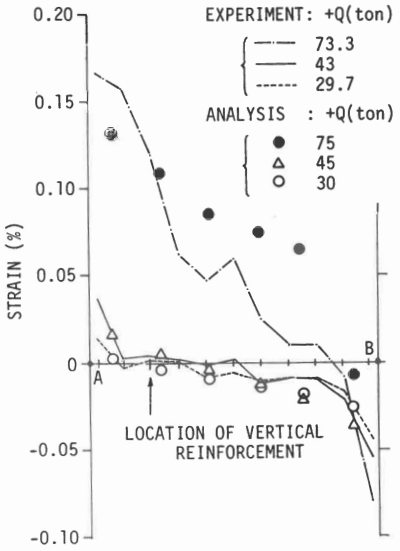

Fig.13 Strain Distribution of Vertical Reinforcement at The Bottom

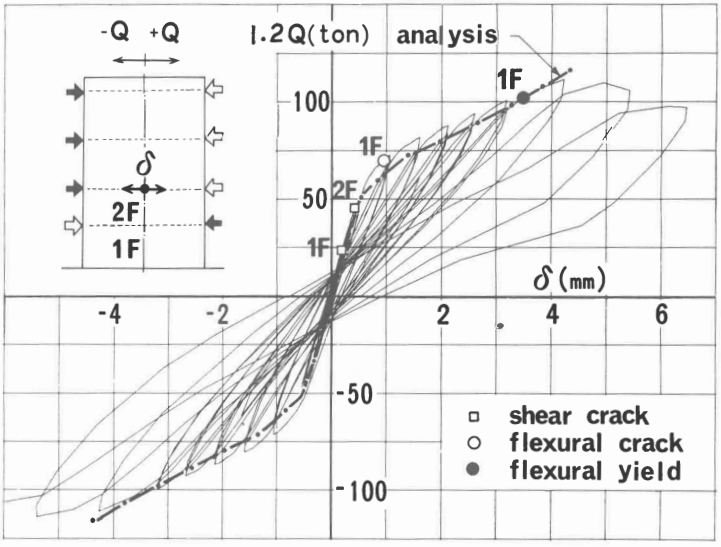

Fig.14 Load-Lateral Displacement